Pre-Filtering of Stimuli for Improved Energy Efficiency in Electrical Neural Stimulation

Francesc Varkevisser*, Amin Rashidi*, Tiago L. Costa*, Vasiliki Giagka*† and Wouter A. Serdijn*‡
Email: {f.varkevisser,amin.rashidi,t.m.l.costa,v.giagka,w.a.serdijn}@tudelft.nl
*Section Bioelectronics, dept. Microelectronics, Delft University of Technology, Delft, The Netherlands
†Technologies for Bioelectronics Group, dept. of System Integration and Interconnection Technologies
Fraunhofer IZM,Berlin, Germany
‡Neuroscience Dept., Erasmus Medical Center, Rotterdam, The Netherlands

***Abstract*—This work proposes a guideline for designing more energy-efficient electrical stimulators by analyzing the frequency spectrum of the stimuli. It is shown that the natural low-pass characteristic of the neuron's membrane limits the energy transfer efficiency from the stimulator to the cell. Thus, to improve the transfer efficiency, it is proposed to pre-filter the high-frequency components of the stimulus. The method is validated for a Hodgkin-Huxley (HH) axon cable model using NEURON v8.0 software. To this end, the required activation energy is simulated for rectangular pulses with durations between 10 μs and 5 ms, which are low-pass filtered with cut-off frequencies of 0.5-50 kHz. Simulations show a 51.5% reduction in the required activation energy for the shortest pulse width (i.e., 10 μs) after filtering at 5 kHz. It is also shown that the minimum required activation energy can be decreased by 11.04% when an appropriate pre-filter is applied. Finally, we draw a perspective for future use of this method to improve the selectivity of electrical stimulation.**

***Index Terms*—neuron modeling, electrical stimulation, neuromodulation, energy transfer efficiency, frequency spectrum**

I. Introduction

Implantable electrical stimulators have proven to be life-changing devices for many patients. Commercially available pacemakers, cochlear implants, and deep brain stimulators are some successful examples. However, there are safety and practical constraints on the energy that can be transferred to and/or stored on such devices [1]. As most of this energy is used by the stimulator circuitry, its power efficiency can play a role in prolonging the functional lifetime of a stimulator device (e.g., battery-powered implants [2]), improving the quality of prosthetic function (e.g., more stimulation sites in visual prostheses [3]), or miniaturizing wireless implants (e.g., smaller receiving aperture in mm-sized implants [4], [5]).

Improving the stimulation energy efficiency requires a good understanding of neural reactions to the stimulation pulses. Activation behavior of neuronal cells has been researched extensively, using a wide variety of analytical and bio-realistic models with different levels of accuracy and complexity [6]–[9]. Hodgkin and Huxley (HH) derived a mathematical description of the non-linear conductance behavior of voltage-gated ion channels in the membrane of a squid giant axon [6]. McNeal's model [7] and the MRG model [8] use single and double cable models, respectively, with HH-channels in the active sections to describe extracellular activation of a myelinated axon fiber. In these models, the HH-like channel mechanisms are tuned to reproduce activation behavior measured in experimental data.

This work is part of the INTENSE project funded by the Dutch Research Council (NWO) under grant number 17619, and the Moore4Medical project funded by the ECSEL Joint Undertaking under grant number H2020-ECSEL-2019-IA-876190

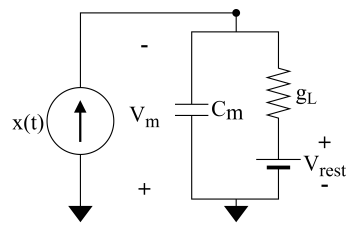

Fig. 1: The linearized membrane model for sub-threshold conditions in the leaky integrate-and-fire model, with membrane capacitance C_m, leakage conductance g_L, rest potential V_{rest}, and the input stimulus x(t).

Even though the aforementioned models can give accurate descriptions of neuron activity, the non-linearity in the ion gate descriptions requires differential equation solvers to predict the response to a given stimulus. Therefore, the computational cost is high, especially in the case of morphologically accurate models or in multi-cell simulations [10]. Simplifying the cell membrane to a linear model makes the prediction of the responses much easier, and a large portion of response phenomena can be accurately explained using the linearized model [11]. A widely used model that assumes linear membrane properties is the Leaky Integrate-and-Fire (LIF) model [9]. In the model, sub-threshold depolarization of the membrane is described by a passive parallel network of a membrane capacitance and a membrane resistance, see Fig. 1. Due to the RC network, the depolarization in sub-threshold conditions as a response to an extracellular stimulus is described by an equivalent membrane time constant, τ_e. When the membrane voltage reaches a predefined threshold value, the model generates an action potential — a spike — and resets the membrane voltage, V_m, to its rest value. This simplified model neglects more complex known properties of cell activation. Nevertheless, it is still widely used to describe cell dynamics in electrical stimulation [12]. For instance, [13] summarizes how τ_e has been used in the literature to estimate strength-, charge-, and energy-duration curves in time-domain analysis.

From a different perspective, the LIF model suggests a first-order low-pass transfer function for the neuron's membrane, which forms the basis of this work. In this paper, we show that the low-pass characteristic of the neuron affects the stimulation

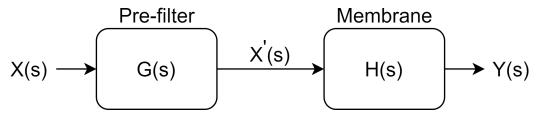

Fig. 2: Diagram of the signal transfer from the stimulator to the neuron.

efficiency dependent on the stimulation waveform. Thus, it is proposed to employ this knowledge to improve the performance of electrical stimulators. In the following sections, the basic concept of the proposed method is explained, and some circuit design guidelines are provided. Then, the potential energy savings are validated using a computational model of an axon fiber. Finally, the conclusion is provided with a discussion on present limitations and future improvements.

II. Basic Concept

The basic concept of this work originates from the fact that the neural membrane has a low-pass characteristic in subthreshold conditions. As a consequence, high-frequency components of a stimulus do not contribute to the depolarization of the cell. Therefore, we propose to pre-filter the stimuli to save energy and reduce the energy delivered to the tissue. As explained in the next section, the losses in the pre-filtering process can be negligible with careful circuit design. Here, the stimuli and the filtering effects are analyzed in the Laplace domain. The total signal transfer function is depicted in Fig. 2, where X(s) is the unfiltered stimulus in the frequency domain, G(s) is the introduced pre-filter for energy saving, X′(s) is the pre-filtered input signal, H(s) represents the low-pass filter (LPF) transfer function of the neuron, and Y(s) is the effective signal delivered to the cell. In this work, both G(s) and H(s) are first-order low-pass filters with corner frequencies $f_{c,G}$ and $f_{c,H}$, respectively. One can derive $f_{c,H}$ from Fig. 1 as $f_{c,H}$ = 1/(2$\pi\tau_e$), with τ_e = C_m/g_L. The energy delivered to the cell and the energy of the input signal are calculated using (1) and (2), respectively. For the case without filtering, G(s) = 1. Consequently, the energy transfer efficiency is defined by (3).

$$E_{out} = \int_{-\infty}^{\infty} |Y(s)|^2 df \tag{1}$$

$$E_{in} = \int_{-\infty}^{\infty} |X'(s)|^2 df \tag{2}$$

$$\eta_E = \frac{E_{out}}{E_{in}} \cdot 100\% \tag{3}$$

If $f_{c,G}$ is chosen such that the total transfer function is dominated by H(s), the input energy (i.e., the energy of X′(s)) is reduced with a small effect on the energy of Y(s). In that case, when the stimulation pulse is short, non-effective high-frequency components can be pre-filtered, which will improve energy efficiency. This is illustrated in Fig. 3 for the example of a pre-filter corner frequency at $f_{c,G}$ = 3·$f_{c,H}$ and a rectangular stimulation pulse with a duration of 1.25·τ_e. In this particular case, η_E is 42.9% and 52.8% for the unfiltered and pre-filtered cases, respectively, indicating an efficiency increase of $(52.8 - 42.9)/42.9 \cdot 100\% = 23.1\%$. It can be

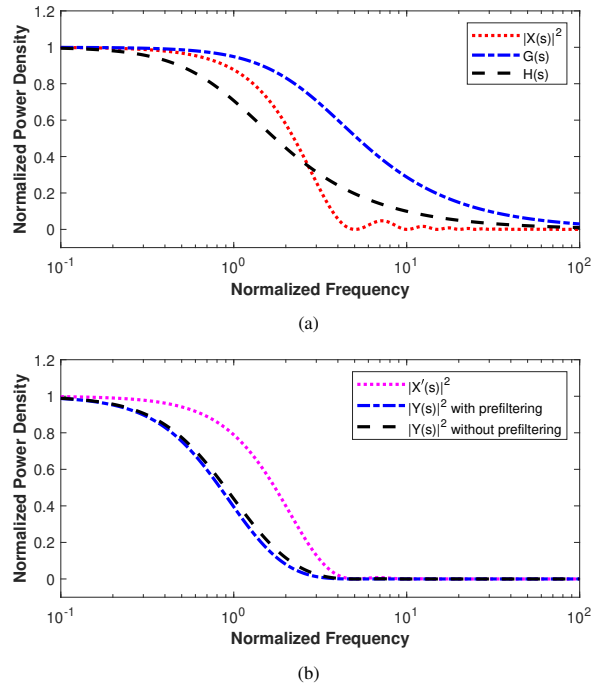

Fig. 3: (a) Spectrum X(s) of rectangular input signal x(t), neuron's bandwidth H(s) and pre-filter bandwidth G(s). (b) Spectrum X'(s) of the pre-filtered input signal x'(t) and the spectra of the resulting output signals with and without pre-filtering. In this example, the frequency axis is normalized to $f_{c,H}$, $f_{c,G}$ = 3·$f_{c,H}$, and the signal is a rectangular pulse with a duration of 1.25·τ_e.

imagined that for long pulses, almost all frequency components fall within the natural bandwidth of the membrane, and thus filtering will have a negligible effect on energy saving. Finally, if the corner frequency of the pre-filter is chosen too low, it will limit the bandwidth of the delivered energy to the tissue and thereby increase the required activation energy.

There are multiple approaches to estimate the neurons' equivalent time constant [14]. The first method uses curve fitting to the Strength-Duration (SD) curve, either to the 'hyperbolic' SD relationship (4) [15] or to the 'logarithmic' SD relationship (5) [9], where I_0 — the rheobase current — is the current threshold for infinitely long pulses, PW the pulse width, and τ_e the equivalent time constant of the cell [14]. Another method uses (6), where Q_0 is the charge threshold for short pulses and I_0 is the rheobase current [14]. Due to the linearization of the model, the time constant will only be an approximation. Therefore, all three time-constant estimation methods are sufficiently accurate.

$$I_{th}(PW) = I_0 \cdot (1 + \frac{\tau_e}{PW}) \tag{4}$$

$$I_{th}(PW) = \frac{I_0}{1 - \exp(-PW/\tau_e)} \tag{5}$$

$$\tau_e = \frac{Q_0}{I_0} \tag{6}$$

III. Circuit Implementation

Based on the previous section, it is possible to achieve system-level energy savings by adequately implementing a

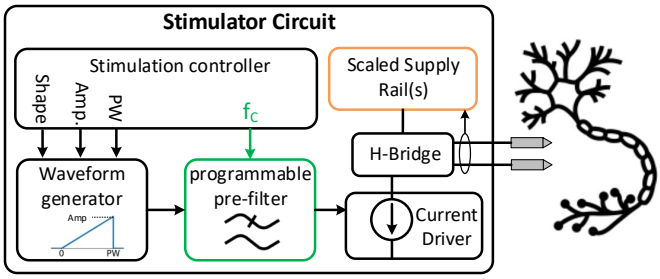

Fig. 4: Block diagram of a current-controlled stimulation output stage with a programmable low-pass filter

pre-filter block before delivering the stimuli to the tissue. Figure 4 illustrates one example of the stimulator circuit implementation in which a stimulation waveform is applied to a programmable low-pass filter before delivering the stimuli through a current driver. Here, it is assumed that the current driver linearly converts the pre-filtered signal to the stimulation current. In case of close-to-ideal loading of the filter (i.e., with either a large input impedance in case of a voltage filter or a small input impedance in case of a current filter), the power consumption of the LFP can be optimized to be negligible. Since the bandwidth of the target neuron is dependent on many factors (e.g., type of nerve, distance from the nerve, orientation with respect to the nerve, the type of tissue in between the electrodes and the nerve, etc.), it is proposed to program the LPF corner frequency (f_c) by the stimulation controller. In other words, it is proposed to apply a more efficient and selective stimulation waveform by introducing a new single stimulation parameter, f_c, in addition to the already known pulse parameters (e.g., duration and amplitudes of the stimuli in anodic and cathodic phases). Notably, the applied stimulation waveform won't be rectangular anymore, and scaling of the supply rail(s) is recommended. The authors have discussed this in [16].

IV. Validation

A. Validation Method

To validate the proposed concept, the current thresholds for different pulse configurations are analyzed in a Hodgkin-Huxley (HH) axon cable model. The axon is modeled in the NEURON v8.0 software [17]. It consists of 101 active nodal sections connected by 100 passive inter-nodal sections, representing a myelinated axon. The active sections contain five HH-like ion channels — transient and persistent sodium and potassium, and A-type potassium (Kv3.1) — which were tuned to the response of a human cortical L5 pyramidal cell in [18]. The model parameters are listed in the Appendix. Extracellular electrical stimulation is modeled for a point-source electrode at a distance of 100μm above the center node of the axon. The extracellular potential along the axon is calculated using (7), where σ is the extracellular conductivity, and r is the distance to the electrode. The potential is applied to each active segment using NEURON's 'extracellular' mechanism. During each simulation step, the potential is scaled according to the amplitude of the applied stimulus.

$$V_e(r) = \frac{1}{4\pi\sigma r} \tag{7}$$

All simulations were executed using implicit Euler integration using a time step of 0.1 μs. A binary search algorithm is employed to determine the threshold amplitude for a pulse configuration to an accuracy of 10^{-2} μA. If the membrane voltage of the outermost node crosses 0 mV, the stimulus is considered supra-threshold. Rectangular, monophasic, cathodic pulses are used as stimuli, with stepped pulse widths (PWs) in steps of 10 μs for the range 10 μs to 500 μs and steps of 100 μs for the range 500 μs to 5 ms.

To estimate the equivalent membrane time constant (τ_e), the strength duration data of the unfiltered pulses (0.1-5 ms in steps of 0.1 ms) is fitted to (4) and (5) using non-linear least squares.

Next, the rectangular pulses were pre-filtered with a 1st-order low-pass filter with corner frequencies ranging from 0.5 to 50 kHz, and the activation thresholds for the resulting pulses were determined for a range of PWs between 10 μs and 5 ms.

The required energy for activation for each pulse configuration is calculated using (8) [19], where $I(t)$ is the applied stimulus at threshold intensity. This calculation assumes a purely resistive load of the stimulator system.

$$E_{th} = \int_0^\infty I(t)^2 dt \tag{8}$$

Finally, we assess the relative optimal energy thresholds between filtered and unfiltered pulses by comparing the minimum required activation energy for both cases using (9), where $E_{fc,\mathrm{x}}$ is the energy curve for the pulses filtered at a frequency of x kHz, and $E_{unfiltered}$ is the energy curve for the unfiltered pulses. The energy curves are compared using their minimal values because the pre-filter alters the effective PW in the time domain.

$$\Delta E_{\mathrm{x}} = \left(\frac{\min(E_{fc,\mathrm{x}})}{\min(E_{unfiltered})} - 1 \right) \cdot 100\% \tag{9}$$

B. Validation Results

The strength-duration curve for the unfiltered pulses in Fig. 5 depicts the minimum required amplitude for a certain PW to excite the neuron. The fitted curves of (4) and (5) are also plotted in Fig. 5. For the exponential fit, τ_e is 0.22 ms, and for the hyperbolic fit, it is 0.18 ms. These correspond to an equivalent corner frequency of the membrane of 723 Hz and 884 Hz, respectively. The estimation of the membrane's cut-off frequency has been used to choose the range of pre-filter corner frequencies in this validation.

The calculated activation energy thresholds for the different pre-filters and PWs are depicted in the energy-duration curves in Fig. 6, where the y-axis is normalized to the minimal value of the unfiltered pulse. The PW depicted in Fig. 6 is the PW of signal $x(t)$ before applying the pre-filter. The corresponding values of ΔE are listed in Table I. In the small pulse width range, it can be seen that filtering with low corner frequencies

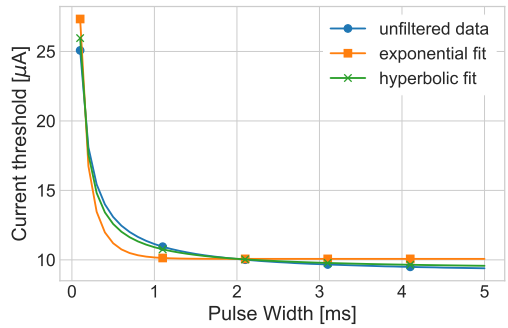

Fig. 5: Strength-Duration curve for the unfiltered pulses, together with the fitted curves for the hyperbolic and exponential relationships [14].

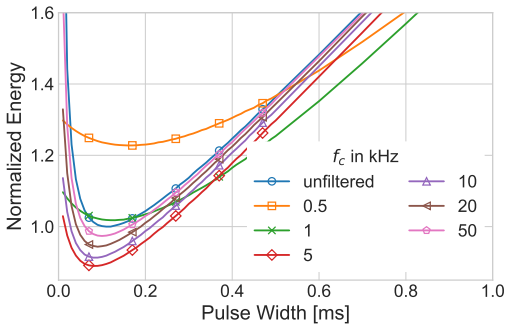

Fig. 6: Energy-Duration relationships for the filtered and unfiltered rectangular pulses, normalized to the optimal value for the unfiltered pulse.

($\leq$1 kHz) increases the activation energy threshold compared to the unfiltered pulses. The required activation energy is minimized when using an f_c of 5 kHz. Further increasing the f_c reduces the energy saving and the energy-duration relationship approaches the unfiltered case. As expected and discussed above, the pre-filtering is more effective for shorter pulses and shows a lower improvement for longer pulses. For example, at a PW of 10 μs, pre-filtering at 5 kHz reduces the required energy by 51.1%, while at 5 ms, the improvement is $<$1%. It should be noted that the filtering changes the effective PW of the pulses in the time domain. After the end of the original pulse, the amplitude decays with $e^{-2\pi f_c t}$.

TABLE I: Relative minimum required energy of filtered pulses

f_c [kHz]	0.5	1.0	5.0	10.0	20.0	50.0
ΔE [%]	22.76	1.79	-11.04	-8.7	-5.63	-2.63

V. Discussion and Conclusion

In this work, we introduced the concept of pre-filtering the stimuli to reduce the required activation energy in electrical stimulation. The foundation of the principle is based on the frequency-domain analysis of the stimulation signals and the linearized cell membrane. The potential energy reduction was validated in a single axon fiber model that included non-linear membrane dynamics.

The presented analysis is focused on energy reduction and is limited to monophasic rectangular stimulation pulses. However, the frequency-domain analysis and pre-filtering could be used for a broader range of analyses and applications, which will be shortly discussed here.

First, the current analysis assumes a purely resistive load to the system. However, it is known that the electrode-tissue interface introduces capacitive components in series with the tissue resistance [20]. In the frequency domain, one could model this as a high-pass filter to enhance the analysis. The location of the corner frequency of this filter depends on multiple factors, including electrode material and geometry. In electrode design for electrical stimulation, capacitive charging should be minimized to prevent harmful electrochemical reactions [20], which would lead to a low corner frequency of the high-pass characteristic.

Second, pre-filtering might be used to increase the selectivity of the stimulation. We focused on a single isolated cell at a fixed distance for the analysis. However, it is known that the equivalent time constant depends on many factors, including axon fiber diameter, electrode size, and the distance from the cell [14]. Careful design and tuning of the pre-filter could reduce activation thresholds for the target cells while increasing the thresholds of non-target cells. In this way, a smaller group of non-target cells will be excited, and therefore the associated adverse effects of stimulation might be reduced.

Third, the effect of pre-filtering should be analyzed for more complex stimuli. For example, frequency-domain filtering of a rectangular pulse does change the effective pulse width in the time domain due to the after-pulse decay. This might affect the usability of the filtering for biphasic pulses and repetitive pulsing. Additionally, the analysis should be extended to non-rectangular or arbitrary waveforms.

Finally, the relation between time- and frequency-domain properties should be explored in more detail. One example is the relation between the total energy and maximum amplitude. From Fig. 3, one can see that even though the effect of pre-filtering on signal Y(s) is small, there is always some degree of modulation. Translating this change to the time domain would be helpful for further understanding the pre-filtering effects. Next to that, it would be useful to identify the optimal ratio between the pre-filter corner frequency and the membrane's time constant.

Appendix

The model parameters are listed in Table II, the membrane dynamics are based on the models presented in [18].

TABLE II: Parameters used in the axon model

Symbol	Description	Value
ρ_a	Axial resistivity	100 $\Omega \cdot$ cm
σ_o	Extracellular conductivity	0.276 S·m^{-1}
d_o	Diameter myelin sections	1.25 μm
d_n	Diameter nodal sections	0.93 μm
L_n	Length nodal sections	1 μm
L_m	Length myelin sections	59 μm
$C_{m,n}$	Membrane capacitance nodal sections	1 μF·cm^{-2}
$C_{m,m}$	Membrane capacitance myelin sections	0.02 μF·cm^{-2}
$R_{m,n}$	Membrane resistance nodal sections	33.3 k$\Omega \cdot$ cm^2
$R_{m,m}$	Membrane resistance myelin sections	1.125 M$\Omega \cdot$ cm^2

REFERENCES

[1] "IEEE standard for safety levels with respect to human exposure to electric, magnetic, and electromagnetic fields, 0 Hz to 300 GHz," *IEEE Std C95.1-2019 (Revision of IEEE Std C95.1-2005/ Incorporates IEEE Std C95.1-2019/Cor 1-2019)*, pp. 1–312, 2019.

[2] H. Lanmüller, M. Bijak, W. Mayr, D. Rafolt, S. Sauermann, and H. Thoma, "Useful applications and limits of battery powered implants in functional electrical stimulations." *Artificial organs*, vol. 21, no. 3, pp. 210–212, 1997.

[3] A. C. Weitz and J. D. Weiland, "Visual Prostheses," in *Neural Computation, Neural Devices, and Neural Prosthesis*. New York, NY: Springer New York, 2014, pp. 157–188. [Online]. Available: http://link.springer.com/10.1007/978-1-4614-8151-5_7

[4] D. K. Piech, B. C. Johnson, K. Shen, M. M. Ghanbari, K. Y. Li, R. M. Neely, J. E. Kay, J. M. Carmena, M. M. Maharbiz, and R. Muller, "A wireless millimetre-scale implantable neural stimulator with ultrasonically powered bidirectional communication," *Nature Biomedical Engineering*, vol. 4, no. 2, pp. 207–222, 2020.

[5] A. Rashidi, S. Hosseini, K. Laursen, and F. Moradi, "STARDUST: Optogenetics, electrophysiology and pharmacology with an ultrasonically powered DUST for parkinson's disease," in *2019 26th IEEE International Conference on Electronics, Circuits and Systems (ICECS)*. IEEE, 2019, pp. 109–110.

[6] A. L. Hodgkin and A. F. Huxley, "A quantitative description of membrane current and its application to conduction and excitation in nerve," *The Journal of Physiology*, vol. 117, no. 4, pp. 500–544, 8 1952. [Online]. Available: https://onlinelibrary.wiley.com/doi/abs/10.1113/jphysiol.1952.sp004764

[7] D. R. McNeal, "Analysis of a Model for Excitation of Myelinated Nerve," *IEEE Transactions on Biomedical Engineering*, vol. BME-23, no. 4, pp. 329–337, 7 1976. [Online]. Available: http://ieeexplore.ieee.org/document/4121058/

[8] C. C. McIntyre, A. G. Richardson, and W. M. Grill, "Modeling the Excitability of Mammalian Nerve Fibers: Influence of Afterpotentials on the Recovery Cycle," *Journal of Neurophysiology*, vol. 87, no. 2, pp. 995–1006, 2 2002. [Online]. Available: https://www.physiology.org/doi/10.1152/jn.00353.2001

[9] L. Lapicque, "Recherches quantitatives sur l'excitation electrique des nerfs traitee comme une polarization," *Journal of Physiol Pathol Générale*, vol. 9, 1907.

[10] S. M. Danner, C. Wenger, S. M. Danner, C. Wenger, and F. Rattay, *Electrical stimulation of myelinated axons: An interactive tutorial supported by computer simulation*. VDM Verlag, 2011, no. March 2018.

[11] J. J. Struijk, "Passive models of excitable cells," in *Neuroprosthetics: Theory and Practice: Second Edition*, 2017, pp. 215–239.

[12] N. Brunel and M. C. Van Rossum, "Lapicque's 1907 paper: From frogs to integrate-and-fire," *Biological Cybernetics*, vol. 97, no. 5-6, pp. 337–339, 12 2007.

[13] J. Reilly and A. M. Diamant, "Theoretical Foundations," in *Electrostimulation: Theory, Applications, and Computational Model*, 2011.

[14] ——, "Excitation Relationships," in *Electrostimulation: Theory, Applications, and Computational Model*, 2011, pp. 23–44.

[15] G. Weiss, "Sur la possibilite de rendre comparables entre eux les appareils servant a l'excitation electrique." *Archives Italiennes de Biologie*, vol. 35, no. 1, pp. 413–445, 1901.

[16] K. Kolovou-Kouri, A. Rashidi, F. Varkevisser, W. A. Serdijn, and V. Giagka, "Energy savings of multi-channel neurostimulators with non- rectangular current-mode stimuli using multiple supply rails," in *2022 44th Annual International Conference of the IEEE Engineering in Medicine & Biology Society (EMBC)*, in press.

[17] N. T. Carnevale and M. L. Hines, *The NEURON Book*. Cambridge: Cambridge University Press, 2006. [Online]. Available: http://ebooks.cambridge.org/ref/id/CBO9780511541612

[18] A. S. Aberra, A. V. Peterchev, and W. M. Grill, "Biophysically realistic neuron models for simulation of cortical stimulation," *Journal of Neural Engineering*, vol. 15, no. 6, p. 066023, 12 2018. [Online]. Available: https://iopscience.iop.org/article/10.1088/1741-2552/aadbb1

[19] A. Wongsarnpigoon and W. M. Grill, "Energy-efficient waveform shapes for neural stimulation revealed with a genetic algorithm," *Journal of Neural Engineering*, vol. 7, no. 4, p. 046009, 8 2010. [Online]. Available: https://iopscience.iop.org/article/10.1088/1741-2560/7/4/046009

[20] D. R. Merrill, M. Bikson, and J. G. Jefferys, "Electrical stimulation of excitable tissue: design of efficacious and safe protocols," *Journal of Neuroscience Methods*, vol. 141, no. 2, pp. 171–198, 2 2005. [Online]. Available: https://linkinghub.elsevier.com/retrieve/pii/S0165027004003826